Treatment of type 2 diabetes mellitus via reversing insulin resistance and regulating lipid homeostasis *in vitro* and *in vivo* using cajanonic acid A

RUIYI YANG[1*], LU WANG[1*], JIE XIE[1], XIANG LI[1], SHAN LIU[1],
SHENGXIANG QIU[2], YINGJIE HU[1] and XIAOLING SHEN[1]

[1]Laboratory of Chinese Herbal Drug Discovery, Institute of Tropical Medicine, Guangzhou University of Chinese Medicine, Guangzhou, Guangdong 510405; [2]Key Laboratory of Plant Resources Conservation and Sustainable Utilization, South China Botanical Garden, Chinese Academy of Sciences, Guangzhou, Guangdong 510650, P.R. China

Abstract. The present study investigated the effects of cajanonic acid A (CAA), extracted from the leaves of *Cajanus cajan* (L.) Millsp with a purity of 98.22%, on the regulatory mechanisms of glucose and lipid metabolism. HepG2 cells transfected with a protein-tyrosine phosphatase 1B (PTP1B) overexpression plasmid were established. The cells, induced with insulin resistance by dexamethasone (Dex) treatment, together with type 2 diabetes mellitus (T2DM) model rats and *ob/ob* mice, were used in the present study. The effects of CAA treatment on the differentiation of 3T3-L1 adipocytes were determined using Oil Red O. The expression levels of insulin signaling factors were detected via reverse transcription-quantitative polymerase chain reaction and western blot analyses. The results revealed that the overexpression of PTP1B contributed to insulin resistance, which was reversed by CAA treatment via inhibiting the activity of PTP1B and by regulating the expression of associated insulin signaling factors. The treatment of cell lines with Dex led to increased expression of PTP1B but decreased glucose consumption, and decreased tyrosine phosphorylation of insulin receptor, insulin receptor substrate 1, and phosphoinositide 3-kinase. Treatment with CAA not only reduced the fasting blood glucose levels and protected organs from damage, but also reduced the serum fasting levels of total cholesterol, triglycerides and low-density lipoprotein cholesterol in the T2DM rats. CAA treatment also inhibited adipocyte differentiation and decreased the mRNA levels of various adipogenic genes. Furthermore, CAA treatment restored the transduction of insulin signaling by regulating the expression of PTP1B and associated insulin signaling factors. Treatment with CAA also reduced the problems associated with hyperglycemia and hyperlipidemia. In conclusion, CAA may be used to cure T2DM via restoring insulin resistance and preventing obesity.

Introduction

Type 2 diabetes mellitus (T2DM) is a metabolic disorder characterized by hyperglycemia, which is mainly associated with insulin resistance and a relative lack of insulin (1). In the case of insulin resistance, impaired insulin signaling transduction inhibits the uptake of circulating glucose by target tissues, which leads to elevated blood glucose levels. A high caloric diet and a sedentary lifestyle are reported to be the primary causes of T2DM in individuals genetically predisposed to this disease (2,3). Furthermore, the glucose metabolic disorders are usually accompanied by lipid metabolic disorders and chronic inflammation (4). Treatment with insulin sensitizers is considered to be beneficial for patients with T2DM and related metabolic disorders, although there is limited evidence available so far. Therefore, the present study investigated the treatment of T2DM via reversing insulin resistance and regulating lipid metabolism.

The insulin-stimulated uptake of glucose in target cells, including the liver, adipose tissues and muscles, is driven by the insulin receptor-mediated signaling transduction pathway (4). The binding of insulin to the membrane-localized α-subunit of the insulin receptor (IR) activates its intracellular β-subunit by tyrosine phosphorylation, which triggers the sequential phosphorylation and activation of downstream signaling molecules, including insulin receptor substrate (IRS), phosphoinositide 3-kinase (PI3K) and AKT. This, in turn, results in the translocation of intracellular glucose transporter (GLUT) vesicles to the plasma membrane for the transportation of

Correspondence to: Professor Xiaoling Shen or Professor Yingjie Hu, Laboratory of Chinese Herbal Drug Discovery, Tropical Medicine Institute, Guangzhou University of Chinese Medicine, 12 Jichang Road, Guangzhou, Guangdong 510405, P.R. China
E-mail: xshen2@gzucm.edu.cn
E-mail: yingjiehu@gzucm.edu.cn

*Contributed equally

extracellular glucose into cells. Numerous factors impair the insulin signaling transduction by suppressing the expression, or by inhibiting the activation of signaling molecules. For example, the protein tyrosine phosphatase non-receptor type 1 (PTPN1) gene can negatively regulate the insulin signaling by dephosphorylating the residues of activated IR via encoding protein-tyrosine phosphatase 1B (PTP1B). The overexpression of PTP1B has been reported to induce insulin resistance and obesity in adipose tissues and skeletal muscles of humans and rodents (5). PTP1B can also inhibit leptin receptor signaling by the dephosphorylation of Janus kinase 2, which is a downstream signal of leptin receptor (6,7). Gene knockout experiments have provided substantial evidence regarding the role of PTP1B in the regulation of insulin signaling and development of obesity. In studies, mice lacking functional PTP1B exhibited increased insulin sensitivity and resistance to obesity. Furthermore, PTP1B-knockout mice fed with high-fat diets were found to be resistant to weight gain and had significantly lower triglyceride levels (8,9). Therefore, PTP1B is a potential target for the treatment of diabetes and obesity-related metabolic disorders; thus the development of PTP1B inhibitors has attracted considerable interest (10-12). The present study aimed to target the treatment of T2DM via reversing insulin resistance by inhibiting PTP1B.

Cajanolic acid A (CAA; Fig. 1A) is a natural stilbene derivative extracted from the leaves of *Cajanus cajan* (L.) Millsp. A previous study reported that CAA can inhibit the activity of PTP1B. Therefore, in the present study, CAA was extracted from the leaves of *C. cajan* (L.) Millsp, and its effects on the regulatory mechanisms of glucose and lipid metabolism were investigated in cell models and animal models of T2DM. The treatment with CAA not only actively reversed PTP1B-mediated and/or dexamethasone (Dex)-induced insulin resistance but also inhibited hormone-induced adipogenesis by inhibiting PTP1B and downregulating peroxisome proliferator-activated receptor-γ (PPARγ). Furthermore, CAA treatment in the present study exhibited significant therapeutic effects on hyperglycemia, hyperlipidemia and obesity in animal models.

Materials and methods

Reagents. The leaves of *C. cajan* (L.) Millsp. were collected from Ledong County (Hainan, China), and CAA was extracted according to the previously reported method (13,14).

Purity assay of CAA. The purity of CAA was analyzed using a Dionex Summit P680 high-performance liquid chromatography (HPLC; Dionex, CA, USA; Fig. 1B) apparatus with an Ecosil HPLC-C18 column (4.6x250 mm, 5 μm), with a mobile phase consisting of acetonitrile: 0.5% aqueous acetic acid (70:30, v/v) at a temperature of 30°C and flow rate 1.0 ml/min. This was then detected at a wavelength of 250 nm (Table I).

Chemicals and reagents. Streptozotocin (STZ), insulin, 3-isobutyl-1-methylxanthine (IBMX), Dex and Oil Red O were purchased from Sigma-Aldrich; EMD Millipore (Billerica, MA, USA). Rosiglitazone maleate tablets (Avandia, an insulin sensitizer) were procured from GlaxoSmithKline (Shanghai, China).

Protein tyrosine phosphatase assay. A PTP1B assay kit (Calbiochem; EMD Millipore) was used to evaluate the effects of CAA on the activity of PTP1B, according to the manufacturer's protocol. The kit included human recombinant PTP1B (residues 1-322) and a phosphopeptide substrate composed of residues 1,142-1,153 of the IRSβ, which requires autophosphorylation to achieve full receptor kinase activation. The free phosphate released was detected to measure the activity of PTP1B.

Cell lines and cell culture. The 3T3-L1 mouse preadipocyte cell line was obtained from Professor WF Fong of Hong Kong Baptist University (Hong Kong, China). The cells were grown and maintained in Dulbecco's modified Eagle's medium (DMEM; Gibco; Thermo Fisher Scientific, Inc., Waltham, MA, USA), containing 4.5 g/l glucose, supplemented with 10% fetal bovine serum (FBS; Gibco; Thermo Fisher Scientific, Inc.), 100 U/ml penicillin and 0.1 mg/ml streptomycin, at 37°C in a humidified atmosphere containing 5% CO_2.

The HepG2 human hepatoblastoma cells were purchased from the Laboratory Animal Center of Sun Yat-Sen University (Guangzhou, China). The cells were maintained in Roswell Park Memorial Institute 1640 medium (RPMI 1640; Gibco; Thermo Fisher Scientific, Inc.), supplemented with 10% FBS, 100 U/ml penicillin and 0.1 mg/ml streptomycin, at 37°C in a humidified atmosphere containing 5% CO_2.

Hormone-induced adipocyte differentiation. In 96-well plates or 6-well plates, the 3T3-L1 preadipocytes were seeded ($3x10^4$ cells/cm^2) and grown to confluence in the growth medium (DMEM with 10% FBS). Subsequently, 2 days after attaining confluence, adipocyte differentiation was induced by incubating cells in a growth medium containing 10 μg/ml insulin, 0.25 μM Dex and 0.5 mM IBMX for 2 days at 37°C. The differentiated cells were incubated in a growth medium containing 10 μg/ml insulin for 2 days, followed by the normal growth medium for 4 days. The media were replaced every 2nd day. Following 8 days of differentiation, over 90% of the cells were differentiated into adipocytes. Fat droplets in adipocytes were visualized using Oil Red O staining, under a light microscope.

Dex-induced insulin resistance in 3T3-L1 and HepG2 cells. Insulin resistance was induced in the HepG2 cells and differentiated 3T3-L1 adipocytes by incubating the cells with 1 μM Dex in their respective growth media for 48 h under the aforementioned cell culture conditions.

Transfection of the PTP1B expression vector into HepG2 cells. The HepG2 cells ($5x10^5$) were plated into six-well plates. On reaching 80% confluence, the cells were maintained in serum-free Opti-MEM I media (Thermo Fisher Scientific, Inc.), and were transfected with 4 μg of expression vector pCMV-PTPN1 (Sino Biological, Beijing, China) containing human PTP1B cDNA and 10 μl Lipofectamine 2000 reagent (Thermo Fisher Scientific, Inc.) premixed with serum-free Opti-MEM I media. The transfected cells were incubated in a CO_2 incubator at 37°C for 4 h, following which the media were replaced with standard DMEM containing 10% FBS. Following transfection for 24 h, the stably transfected cells
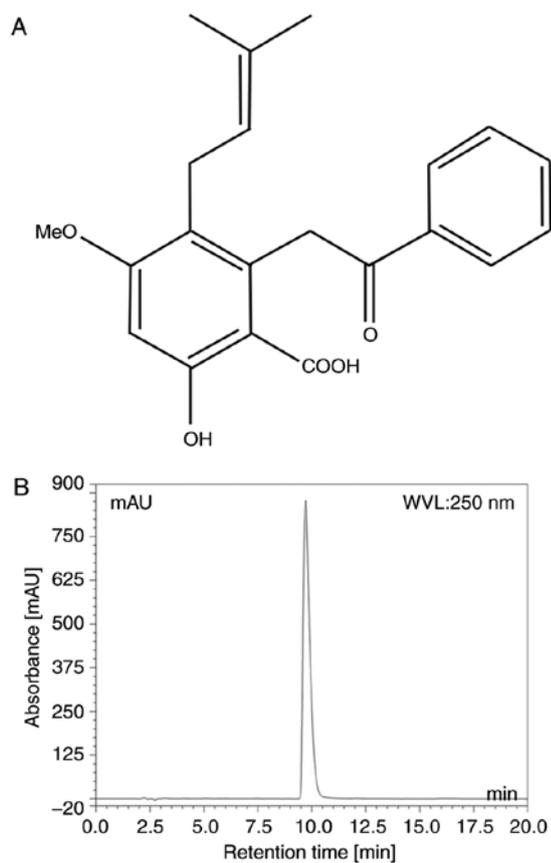
Figure 1. CAA. (A) Structure of CAA and (B) microcolumn reversed phase high-performance liquid chromatography of CAA. CAA, cajanonic acid A.

Table I. Parameters of high-performance liquid chromatography of cajanonic acid A purity detection.

No.	Retention time (min)	Height	Area	Relative area (%)
1	2.17	2.633	0.201	0.06
2	2.25	3.091	0.340	0.11
3	2.54	1.895	0.511	0.16
4	2.81	3.020	0.213	0.07
5	2.93	0.311	0.019	0.01
6	3.11	4.186	1.940	0.61
7	3.25	0.722	0.057	0.02
8	4.07	1.069	0.143	0.04
9	4.24	0.407	0.047	0.02
10	4.75	0.138	0.013	0.00
11	5.04	0.889	0.182	0.06
12	5.23	0.520	0.074	0.02
13	6.01	0.395	0.065	0.02
14	7.44	0.570	0.109	0.03
15	9.72	853.547	312.24	98.22
16	12.1	0.978	0.405	0.13
17	21.91	0.590	0.535	0.17
18	30.70	1.072	0.807	0.25
19	30.73	0.005	0.000	0.00
Total	161.00	876.038	317.901	100

were collected and screened using 150 μg/ml hygromycin (Roche Diagnostics, Basel, Switzerland).

Glucose consumption assay. In 96-well plates, differentiated 3T3-L1 adipocytes or 8,000 adhered HepG2 cells in 100 μl fresh media were incubated at 37˚C with 6.25, 12.5 or 25 μM CAA for either 24 or 48 h, in a CO_2 incubator. The glucose residues in the cell culture media were measured using a glucose oxidase assay kit (Huili Biotechnologies, Changchun, China).

Animal care and diabetic rat models. A total of 50 male Sprague-Dawley (SD) rats (4-weeks-old, weighing 60-80 g) were purchased from the Laboratory Animal Center of Guangzhou University of Chinese Medicine (certificate no. 0040568). Male adult *ob/ob* mice (5-weeks-old, weighing 30-40 g, stock no. 000632) were purchased from the Jackson ImmunoResearch Laboratories, Inc. (West Grove, PA, USA).

The animals were allowed free access to food and filtered tap water *ad libitum,* and were maintained at 23±2˚C with 50-70% relative humidity and 12-h dark/light cycles under pathogen-free conditions. All experiments were approved by the Animal Ethics Committee of Guangzhou University of Chinese Medicine (Guangzhou, China; no. SYXY2008-0001) and were performed following the Animal Care and Use guidelines set by the committee.

Symptoms of T2DM were induced in 42 male SD rats by feeding a high-fat diet (60% standard diet, 20% lard, 10%

yolk powder and 10% saccharose) for 8 weeks. The rats were fasted for 16 h and subsequently injected intraperitoneally with 30 mg/kg STZ. Meanwhile, the other 8 rats fed with a standard diet served as a normal control (NC), and these rats were administered with an equivalent volume of 0.1 M citrate buffer (pH 4.4) instead of STZ. At 2 weeks post-STZ injection, the rats were subjected to fasting for 14 h, and the fasting blood glucose (FBG) levels were measured from the caudal vein using an Accu-Chek active blood glucose monitoring meter (Roche Diagnostics). The animals with FBG levels of 12-28 mM, and with symptoms of polyuria and polydipsia, were considered diabetic.

CAA treatment. The antidiabetic properties of CAA were investigated by randomly dividing 24 diabetic rats into three groups (n=8/group) according to their FBG and bodyweight (BW), and were administered with 10 mg/kg/day (a minimum effective dosage, based on our previous experiments, data not shown) of CAA or an equivalent volume of vehicle (5% Tween-80 and 5% DMSO in water) intraperitoneally, or 4 mg/kg/day of Avandia (positive control) orally for 4 weeks. All the diabetic rats continued to receive the high-fat diet during the experiment. Furthermore, 12 male adult *ob/ob* mice that had grown to 12 weeks of age were randomly divided into two groups (n=6/group), which received CAA (8 mg/kg/day intraperitoneally, which was identified as the minimum effective dosage based on our previous experiments (data not shown) or an equivalent volume of vehicle (5% Tween-80 and 5% DMSO in water) for 12 days. The FBG levels and BW were

measured on day 0 (prior to the first treatment), and days 5 and 12 following the final treatment. In addition, eight healthy rats of the same age, fed on the standard diet, were used as the normal control (NC) group.

Oral glucose tolerance test (OGTT) and lipid metabolism assessment. OGTTs were performed at the start and the end of drug treatment, respectively. Animals fasted for 12 h were orally administered 2 g/kg of glucose; plasma glucose levels at 0, 30, 60 and 120 min following glucose administration were measured from the caudal vein using a blood glucose monitoring meter. At the end of experiment, blood samples from the aorta abdominalis were centrifuged at 2,500 x g for 10 min at 4˚C, and the fasting serum levels of triglycerides (TG), total cholesterol (TC), high-density lipoprotein cholesterol (HDL-C), low-density lipoprotein cholesterol (LDL-D), urea, uric acid, creatinine, aspartate transaminase (AST), alanine transaminase (ALT) and glucose (FSG) were measured with an AU5400 automatic analyzer (Olympus Corporation, Tokyo, Japan). The fasting insulin levels of serum (FINS) were measured using a rat insulin ELISA kit (R&D Systems, Inc., Minneapolis, MN, USA). The homeostatic model assessments for insulin resistance index and β-cell function index (HOMA-IR and HOMA-β, respectively) were calculated to evaluate β-cell function (15), using the following equations: HOMA-IR = FSG x FINS/22.5; HOMA-β = 20 x FINS/(FSG-3.5).

The livers were weighed, and the liver to body weight (LW/BW) ratio was calculated to evaluate liver swelling. Then tissues were then fixed in paraformaldehyde (4%) for 24 h, and 4-μm sections were used for further staining following embedding with paraffin. The pancreas, liver and kidneys were analyzed histopathologically using hematoxylin and eosin stain, with 0.1% hematoxylin for 6 min at room temperature and 0.5% eosin for 2 min at room temperature, under a light microscope.

Reverse transcription-quantitative polymerase chain reaction (RT-qPCR) analysis. Total RNAs were isolated from the cells and reverse transcription was performed using the RNAprep Cell/Bacteria kit (Tiangen Biotech Co., Ltd., Beijing, China) and ReverTra Ace qPCR RT kit (Toyobo Co., Ltd., Osaka, Japan) respectively, according to manufacturer's protocols. The mRNA levels of the target genes were measured using qPCR analysis with Thunderbird SYBR qPCR mix (Toyobo Co., Ltd.). For performing the amplification, 12.5 μl of SYBR qPCR mix, 1X ROX reference, 0.3 μM of primer pairs each, 2.5 μl of 10-fold diluted cDNA were mixed, and the sterile distilled water finally supplemented to 25 μl total volume. The quantitative assay was evaluated in a 7500 Real-time PCR system (Applied Biosystems; Thermo Fisher Scientific, Inc.) under 2-Step Cycling (95˚C for 1 min hold, 40 cycles of 95˚C for 15 sec and 60˚C for 40 sec). β-actin was used as the inner reference gene, and the relative gene expression was calculated based on $2^{-\Delta\Delta Cq}$ method (16). The primers designed for amplifying target genes are listed in Tables II and III.

Western blot analysis. The cells were harvested and lysed with an ice-cold cell lysis buffer for western and IP (Beyotime Institute of Biotechnology, Shanghai, China), which contained the protease inhibitor PMSF at final concentration of 1 mM.

Table II. Primers designed for quantitative amplification in humans.

Gene	Primer sequence (5'-3')	Length (bp)
PTP1B-F	AGCCAGTGACTTCCCATGTAG	257
PTP1B-R	TGTTGAGCATGACGACACCC	
IRS1-F	GGAAGAGACTGGCACTGAGG	199
IRS1-R	CTGACGGGGACAACTCATCT	
IRS2-F	CAACACCTACGCCAGCATTGA	107
IRS2-R	CTCTGACATGTGACATCCTGGTGA	
GSK3β-F	AACTGCCCGACTAACACCAC	268
GSK3β-R	TGCAGAAGCAGCATTATTGG	
GLUT1-F	CGGGCCAAGAGTGTGCTAAA	283
GLUT1-R	TGACGATACCGGAGCCAATG	
β-actin-F	TGGCACCCAGCACAATGAA	186
β-actin-R	CTAAGTCATAGTCCGCCTAGAAGCA	

F, forward primer; R, reverse primer; PTP1B, protein-tyrosine phosphatase 1B; IRS, insulin receptor substrate; GSK3β, glycogen synthase kinase-3β; GLUT1, glucose transporter 1.

Table III. Primers designed for quantitative amplification in mice.

Gene	Primer sequence (5'-3')	Length (bp)
PTP1B-F	TTCAAAGTCCGAGAGTCAGG	236
PTP1B-R	ACAGCCAGGTAGGAGAAGC	
PPARγ-F	TGTCGGTTTCAGAAGTGCCTTG	122
PPARγ-R	TTCAGCTGGTCGATATCACTGGAG	
C/EBPα-F	TGCGCAAGAGCCGAGATAAAG	115
C/EBPα-R	TCACGGCTCAGCTGTTCCAC	
ADD1/S-F	TACTTCTTGTGGCCCGTACC	129
ADD1/S-R	TCAGGTCATGTTGGAAACCA	
FAS-F	CTGAGGACTTCCCAAACGG	228
FAS-R	TGGCCTGATGAAACGACAC	
AP2-F	AGCGTAAATGGGGATTTGGT	178
AP2-R	TCGACTTTCCATCCCACTTC	
LPL-F	GCCCAGCAACATTATCCAGT	168
LPL-R	GGTCAGACTTCCTGCTACGC	
β-actin-F	CATCCGTAAAGACCTCTATGCCAAC	171
β-actin-R	ATGGAGCCACCGATCCACA	

F, forward primer; R, reverse primer; PTP1B, protein-tyrosine phosphatase 1B; PPARγ, peroxisome proliferator-activated receptor γ; C/EBPα, CCAAT enhancer binding protein α; ADD1/S, adipocyte determination and differentiation factor 1/sterol regulatory element binding protein 1c; FAS, fatty acid synthase; AP2, adipocyte fatty acid-binding protein 2; LPL, lipoprotein lipase.

The total concentration of extracted proteins was determined using an Enhanced BCA Protein Assay kit (Beyotime Instittue

Table IV. List of antibodies for western blot analysis.

Protein	Vendor	Cat. no.	Dilution	Incubation
PTP1B	Abcam (Cambridge, UK)	ab52650	1:1,500	RT, 1 h
p-IR	Abcam	ab5681	1:2,000	RT, 1 h
p-IRS1	Abcam	ab66153	1:3,000	RT, 1 h
p-PI3K	Abcam	ab182651	1:2,000	RT, 1 h
p-AKT	Santa Cruz Biotechnology, Inc. (Dallas, TX, USA)	sc-81433	1:2,000	RT, 1 h
GLUT1	Abcam	ab115730	1:2,500	RT, 1 h
GLUT4	Santa Cruz Biotechnology, Inc.	sc-53566	1:2,000	RT, 1 h
GAPDH	Aksomics (Shanghai) Biotechnology Co., Ltd. (Shanghai, China)	KC-5G5	1:10,000	RT, 1 h
HRP Goat anti-Rabbit IgG	Boster Biological Technology Co., Ltd. (Wuhan, China)	BA1054	1:20,000	RT, 40 min
HRP Goat anti-Mouse IgG	Boster Biological Technology Co., Ltd.	BA1051	1:20,000	RT, 40 min

PTP1B, protein-tyrosine phosphatase 1B; IR, insulin receptor; IRS, insulin receptor substrate; PI3K, phosphoinositide 3-kinase; AKT, serine/threonine protein kinase; GLUT1, glucose transporter 1; GLUT4, glucose transporter 4; p-, phosphorylated; RT, room temperature.

of Biotechnology). A total of 20 μg of the extracted proteins were subjected to 10% SDS-PAGE, and electrotransferred onto a PVDF membrane (Merck Millipore, Darmstadt, Germany) at 300 mA. The membrane was incubated with corresponding primary and secondary antibodies (Table IV), successively. The blots were detected using a Kodak film developer (Fujifilm, Tokyo, Japan). Protein levels were quantified by densitometry analysis using Image-pro plus 6.0 software (Media Cybernetics, Inc., Rockville, MD, USA), GAPDH was used as endogenous control.

Statistical analysis. The data are presented as the mean ± standard error of the mean. Data on relating to the expression of PTP1B and glucose consumption in the cells following transfection with the PTP1B overexpression plasmid, glucose consumption following DEX treatment and residual glucose concentration following CAA treatments were analyzed using a t-test in Microsoft Excel 2013 (Microsoft Corporation, Redmon, WA, USA). The remaining data were analyzed using one-way analysis of variance (SPSS 19.0, IBM Corp., Armonk, NY, USA). $P<0.05$ was considered to indicate a statistically significant difference. All experiments were performed three times (n=3).

Results

CAA inhibits the activity of PTP1B. The purity of the CAA extracted from the leaves of *C. cajan* (L.) Millsp in the present study was determined to be 98.22%. The protein tyrosine phosphatase assay for PTP1B activity showed that CAA effectively reduced the PTP1B-catalyzed dephosphorylation of the phosphopeptide substrate, with a half maximal inhibitory concentration of 63.19 μM. Specifically, treatment with 200 μM CAA decreased the activity of PTP1B to 1.8%, compared with that of in the blank (0 μM) group (Fig. 2).

PTP1B regulates glucose consumption in HepG2 hepatoblastoma cells. Previous studies have reported that PTP1B inhibits
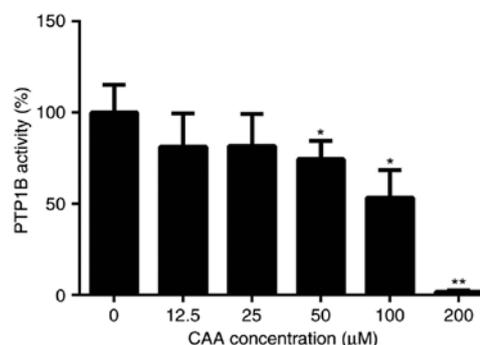
Figure 2. CAA inhibits activity of PTP1B. All results are expressed as the mean ± standard error of the mean (n=6). *$P<0.05$ and **$P<0.01$, compared with controls without CAA. PTP1B, protein-tyrosine phosphatase 1B; CAA, cajanonic acid A.

the activity of insulin by catalyzing the dephosphorylation of the IR and other key proteins in the insulin signaling pathway (6,7). RT-qPCR analysis of the cells transfected with the PTP1B overexpression plasmid (hereafter referred to as HepG2/PTP1B cells), was performed to examine the effects of the expression of PTP1B on insulin signaling pathway. The HepG2/PTP1B cells exhibited increased expression levels of PTP1B by ~4-fold, compared with that of non-transfected HepG2 cells (Fig. 3A). In addition, as shown in Fig. 3B-E, insulin stimulation increased the transcript levels of *IRS1* and *GLUT1* by 1- and 2-fold in the NC group, but decreased the levels of *IRS1* by 58%, with no change in *GLUT1* in the HepG2/PTP1B cells. No significant differences were observed in the expression levels of IRS2 or GSK3β in response to insulin stimulation between the cells with either basal or the overexpressed PTP1B. At the protein level, the HepG2/PTP1B cells exhibited increased expression levels of PTP1B by 1.5-fold, compared with that of the non-transfected HepG2 cells (Fig. 3F and G).

A glucose consumption assay was performed to assess the effects of the overexpression of PTP1B on cellular insulin
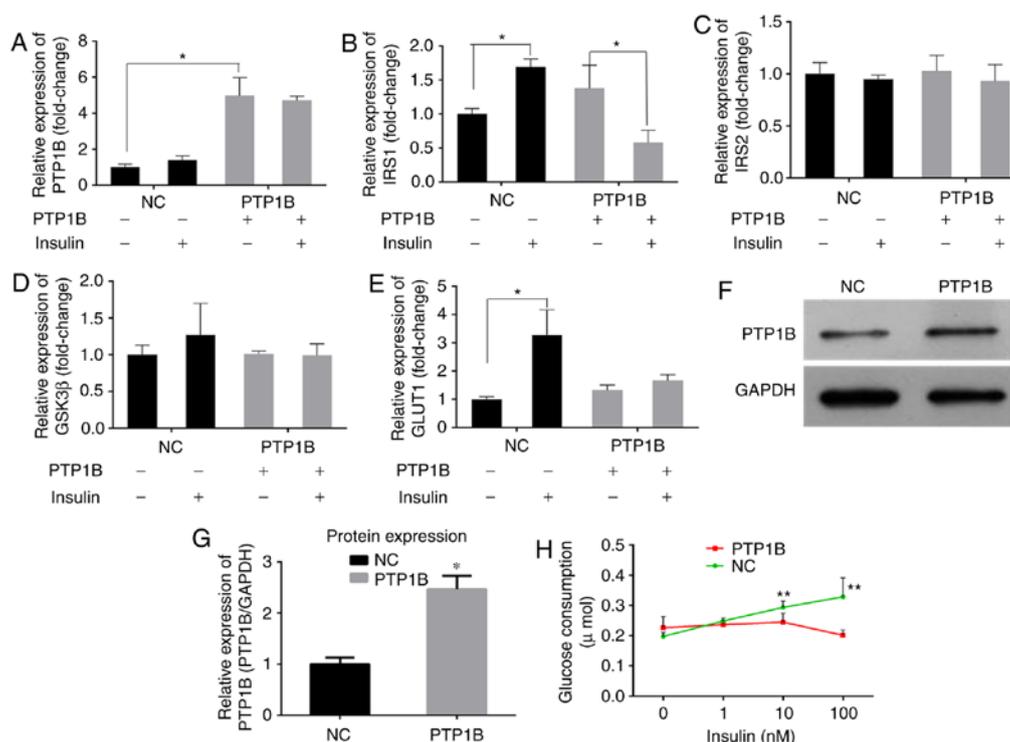
Figure 3. Overexpression of PTP1B induces insulin resistance in HepG2 cells. The expression levels of (A) PTP1B, (B) IRS1, (C) IRS2, (D) GSK3β and (E) GLUT1 involved in insulin signaling were monitored using reverse transcription-quantitative polymerase chain reaction analysis. HepG2 cells transfected with PTP1B vectors were treated with 0 and 100 nM insulin. (F and G) Protein expression levels of PTP1B from western blots. (H) Glucose consumption in HepG2 with PTP1B and insulin (0, 1, 10, 100 nM) intervention for 24 h. All results are expressed as the mean ± standard error of the mean (n=3-6). *P<0.05, **P<0.01, vs. NC without insulin. PTP1B, protein-tyrosine phosphatase 1B; IRS, insulin receptor substrate; GSK3β, glycogen synthase kinase-3β; GLUT1, glucose transporter 1; NC, normal control.

sensitivity. As shown in Fig. 3H, the glucose consumption of NC cells following incubation with insulin (1, 10 or 100 nM) increased but did not exhibit any significant change in the PTP1B overexpressed cells. These results indicated that, although the cells overexpressing PTP1B exhibited basal glucose consumption roughly equivalent to that of HepG2 cells, they exhibited resistance towards insulin-stimulated glucose uptake.

CAA reverses insulin-resistance in HepG2 cells. CAA treatment increased the insulin-stimulated mRNA levels of *IRS1*, *IRS2* and *GLUT1* in the HepG2/PTP1B cells in a dose-dependent manner. Specifically, the mRNA levels of *IRS1*, *IRS2* and *GLUT1* were 4, 1 and 1.6 times higher in the cells treated with 25 *μ*M CAA, respectively, than those in the control (Fig. 4A). Although CAA treatment did not affect the expression of *PTP1B* at the mRNA level (Fig. 4A), it significantly suppressed the protein levels of PTP1B (Fig. 4B), which indicated that the inhibitory effects of CAA on the expression of PTP1B occurred at the post-transcriptional level. Additionally, the CAA treatment-assisted inhibition of PTP1B led to increases in the expression of GLUT1, and the phosphorylation of insulin-stimulated IR, IRS1, PI3K and AKT (Fig. 4B). The effects of CAA on the resistance of HepG2/PTP1B cells to insulin were investigated using 6.25, 12.5 and 25 *μ*M of CAA. Compared with the control group (without CAA treatment), CAA-treated groups (Fig. 4C) exhibited time and dose-dependent increases in insulin-stimulated glucose consumption of the cells. These data suggested that CAA treatment in the present study not

only inhibited PTP1B, but also upregulated the expression and activity of insulin signal transduction factors, and thus reversed the hepatocellular insulin resistance induced by the overexpression of PTP1B.

CAA improves Dex-impaired insulin-stimulated glucose consumption in HepG2 cells and 3T3-L1 adipocytes. The ability of CAA to modulate artificially induced insulin resistance by Dex was assessed. The HepG2 cells and mature 3T3-L1 adipocytes were treated with 1 *μ*M Dex in a medium containing 10% FBS for 48 h, followed by treatment with CAA in a medium containing 0.5% FBS and 10 nM insulin for either 24 or 48 h. The results revealed that the glucose consumption was reduced by ~30% (Fig. 5A, CAA=0) and 18% (Fig. 5B, CAA=0) in the HepG2 cells and 3T3-L1 adipocytes following 48 h of Dex treatment, respectively. In addition, marginally increased expression of PTP1B, decreased expression of GLUT1 (Fig. 5C) and GLUT4 (Fig. 5D) and decreased phosphorylation of IR, IRS1, PI3K and AKT were observed (Fig. 5C and D). These results indicated that 1 *μ*M Dex induced cellular insulin resistance by inactivating the insulin signaling pathway.

By contrast, treatment with CAA did not increase the glucose consumption of cells not exposed to Dex, but markedly increased glucose consumption of the Dex-induced insulin-resistant cells in a dose-dependent manner. As presented in Fig. 5, 25 *μ*M CAA treatment restored the glucose consumption in Dex-treated cells to the normal levels (Fig. 5A and B).
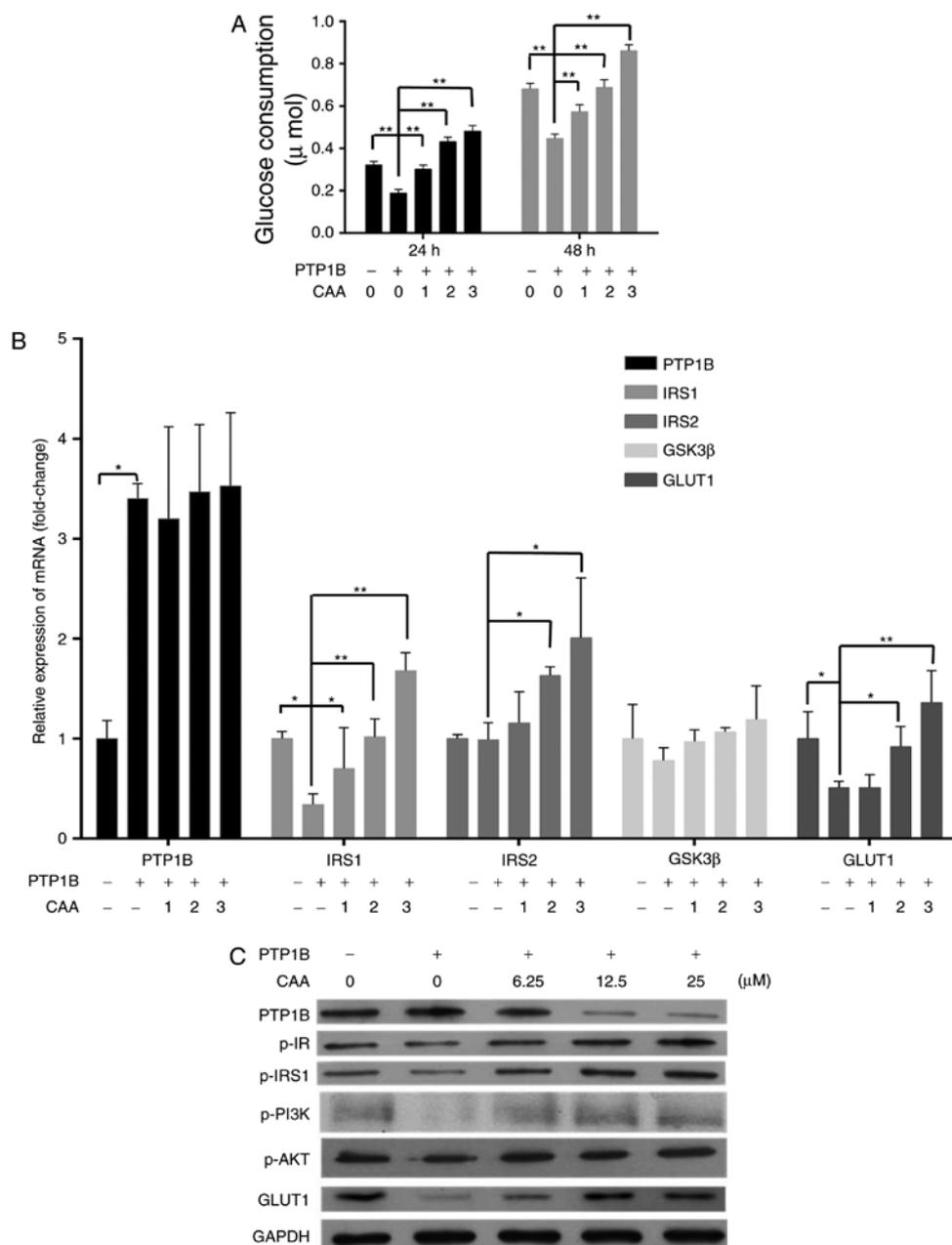
Figure 4. CAA reverses the insulin resistance induced by overexpression of PTP1B in HepG2 cells. (A) Expression of insulin signaling genes as analyzed using reverse transcription-quantitative polymerase chain reaction analysis. (B) Expression and phosphorylation of insulin signaling proteins analyzed using western blot analysis with CAA (0, 6.25, 12.5 and 25 μM) and PTP1B intervention. All results are expressed as the mean ± standard error of the mean (n=3-6). (C) Glucose consumption in response to insulin with CAA. *P<0.05 and **P<0.01. 1, 2 and 3 indicate CAA concentrations of 6.25, 12.5 and 25 μM, respectively. PTP1B, protein-tyrosine phosphatase 1B; IRS, insulin receptor substrate; GSK3β, glycogen synthase kinase-3β; GLUT1, glucose transporter 1; PI3K, phosphoinositide 3-kinase; IR, insulin receptor; AKT, serine/threonine protein kinase; CAA, cajanonic acid A; p-, phosphorylated.

The results of the western blot analysis revealed that CAA treatment downregulated the expression of PTP1B, but upregulated the expression of GLUT1 or GLUT4, and increased the levels of phosphorylated IR, IRS1, PI3K and AKT (Fig. 5C and D), which indicated the promotion of glycometabolism in the Dex-treated cells treated with CAA.

Therapeutic effects of CAA in an SD rat model of T2DM. The present study also investigated the effects of CAA treatment on the modulation of insulin resistance in SD rats fed on high-fat diet, having STZ-induced T2DM. Avandia (tosiglitazone), a clinically used insulin sensitizer, was used as the positive control. As shown in Fig. 6A and B, over a 4-week experimental period, the BW of the normal rats steadily increased from 372±22 to 424±29 g, but their FBG levels remained considerably low (≤7.0 mM). By contrast, the FBG levels of the vehicle-treated diabetic rats increased from 22.5±1.6 to 26.8±1.7 mM, whereas their BW decreased from 357±18 to 346±21 g, which indicated a severe diabetic condition. Compared with the diabetic rats treated with vehicle, the rats treated with CAA or Avandia exhibited a marginally higher BW (Fig. 6A), markedly lower FBG levels (Fig. 6B) and improved oral glucose tolerance (Fig. 6C).
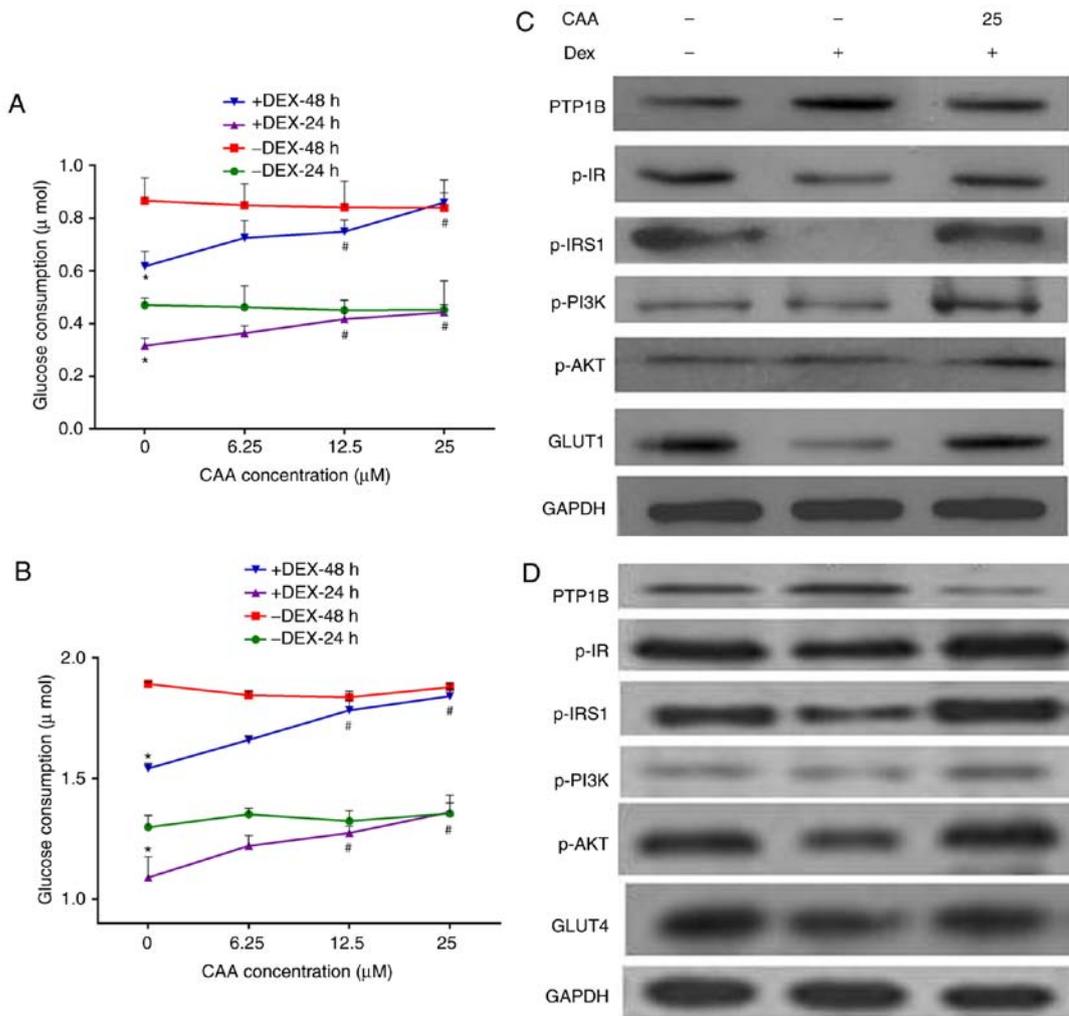
Figure 5. CAA improves the insulin sensitivity impaired by Dex in HepG2 cells and 3T3-L1 adipocytes. (A) Glucose consumption in response to insulin in the HepG2 cell line. (B) Glucose consumption in response to insulin in 3T3-L1 adipocytes. (C) Expression and phosphorylation of insulin signaling proteins in HepG2 cells analyzed using western blot analysis. (D) Expression and phosphorylation of insulin signaling proteins in 3T3-L1 adipocytes analyzed using western blot analysis. Prior to CAA treatment, the cells were incubated with 0 (-) or 1 μM (+) Dex for 48 h. For glucose consumption experiments, the cells were treated with CAA (0, 6.25, 12.5 and 25 μM) in 0.5% fetal calf serum and 10 nM insulin for 24 or 48 h. For western blot analysis, the cells were treated with 25 μM CAA for 24 h followed by 100 nM insulin for 30 min. All results are expressed as the mean ± standard error of the mean (n=3-6). $^{*}P<0.05$, vs. cells without DEX treatment; $^{\#}P<0.01$, vs. cells without CAA treatment. PTP1B, protein-tyrosine phosphatase 1B; IR, insulin receptor; IRS, insulin receptor substrate; GLUT1, glucose transporter 1; GLUT4, glucose transporter 4; PI3K, phosphoinositide 3-kinase; AKT, serine/threonine protein kinase; CAA, cajanonic acid A; p-, phosphorylated; Dex, dexamethasone.

Lifestyle-induced hyperglycemia is often accompanied by lipid metabolic disorders. Individuals with abnormal blood lipid profiles are more vulnerable to diabetes; improvement in lipid metabolism can assist in alleviating the diabetic condition (17). Therefore, the present study further assessed lipid metabolism in the experimental rats. The vehicle-treated T2DM rats exhibited significantly elevated serum levels of TC (P<0.01), TG (P<0.01) and LDL-C (P<0.001), which indicated dyslipidemia compared with the normal group. By contrast, CAA treatment significantly reduced the levels of lipid regulatory effects, including TG (P<0.05), TC (P<0.01) and LDL-C (P<0.001), in the T2DM rats, similar to the rats treated with Avandia (Fig. 7A). The levels of FINS remained unchanged in all groups (Fig. 7B), which suggested that CAA, as with Avandia, did not stimulate insulin secretion. In addition, as shown in the HOMA-IR and HOMA-β data (Fig. 7B), CAA and Avandia had a protective effect on β-cell function.

CAA mitigates the organ damage induced by hyperglycemia and hyperlipidemia. Hyperglycemia and hyperlipidemia induce dysfunctions and damage in important body organs, including the pancreas, liver and kidneys. As shown in Fig. 7, in addition to impaired β-cell function (Fig. 7B), the vehicle-treated diabetic rats exhibited significantly (P<0.05) higher serum levels of AST, ALT (Fig. 7C), urea and creatinine (Fig. 7D), and increased liver to body weight ratio (P<0.001) (Fig. 7C), all of which are indicators of liver swelling, and liver and kidney dysfunction. Furthermore, the histopathological analysis of these rats revealed significant damages in the pancreas (Fig. 8A-D), including acinar atrophy, interstitial widening, steatosis, interstitial fibers and inflammation in the pancreatic islets, in the liver (Fig. 8E-H), including severe spotty necrosis of liver cells and fatty degeneration, and the kidney (Fig. 8I-L), including tubular dilatation, diffuse thickening of the basement membrane and a large number of glycogen vacuoles on proximal tubular epithelial cells.
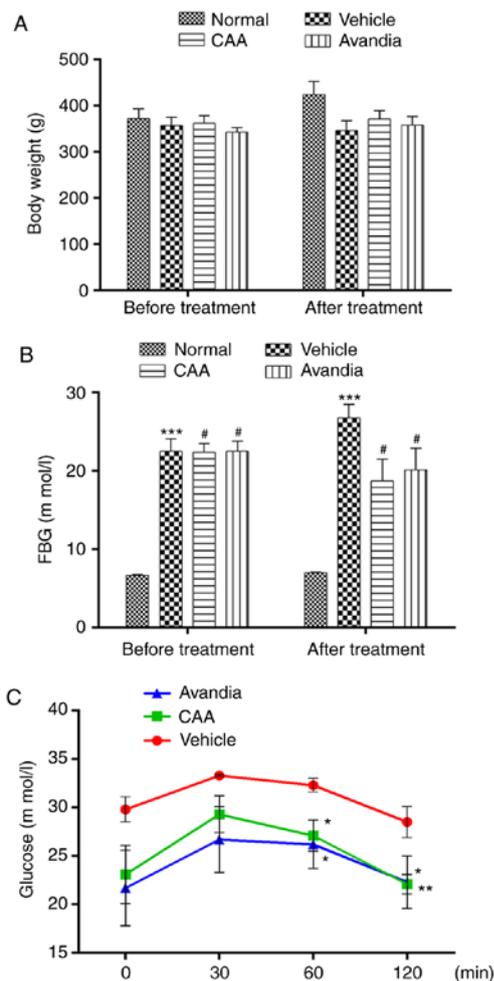
Figure 6. CAA improves the diabetic condition of type II diabetes mellitus Sprague-Dawley rats. Rats were treated with 10 mg/kg/day CAA, 4 mg/kg/day Avandia, or vehicle for 4 weeks. (A) Body weight and (B) FBG were measured prior to (0 weeks) and following (4 weeks) the experiment. (C) Oral glucose tolerance tests were performed following the final treatment. Data are expressed as the mean ± standard error of the mean (n=8). [*]P<0.05, [**]P<0.01 and [***]P<0.001, vs. normal rats; [#]P<0.05, vs. vehicle-treated rats. CAA, cajanonic acid A; FBG, fasting blood glucose.

Following CAA treatment, insulin secretion remained stable, whereas the serum levels of glucose (P<0.05), AST (P<0.05) and ALT (P<0.01) decreased significantly in the T2DM SD rats. Treatment with 10 mg/kg/day CAA intraperitonally also mitigated the damage to the pancreas, liver and kidney in the T2DM SD rats, showing similar results as Avandia in increasing insulin sensitivity, and improved β-cell and liver function (Figs. 7B-D and 8).

Effects of CAA in ob/ob mice. The efficacy of CAA in congenital obese and hyperglycemic *ob/ob* mice was further investigated. As shown in Fig. 9A and B, CAA (8 mg/kg/day intraperitoneally for 12 days) caused time-dependent reductions in BW and FBG, compared with those of the vehicle treated groups (P<0.01). Treatment with CAA significantly decreased FBG on day 5 and day 12 (Fig. 9A), and BW on day 12 (Fig. 9B). In addition, CAA treatment significantly improved the oral glucose tolerance (Fig. 9C and D). Blood glucose was measured at 0, 30, 60 and 120 min on days 0 and 12. On day 12, following 120 min of oral glucose tolerance

tests, the blood glucose level of the CAA-treated group was 17.5±2.5 mM, whereas that of the vehicle treated group reached 28.5±1.4 mM (P<0.01), which indicated the potential of CAA in treating obesity and obesity-induced metabolic disorders.

CAA inhibits hormone-induced adipocyte differentiation by inhibiting the expression of adipogenic genes. To understand the mechanism of action of CAA in *ob/ob* mice, the effects of CAA on hormone-induced adipogenesis were examined in murine 3T3-L1 preadipocytes. The Oil Red O staining results showed that the treatment comprising a mixture of Dex, IBMX and insulin successfully induced the differentiation of 3T3-L1 preadipocytes (Fig. 10A) into mature adipocytes (Fig. 10B). The addition of 150, 100, 75 or 50 μM CAA resulted in a dose-dependent reduction in Oil Red O staining, which indicated that treatment with CAA inhibited adipocyte differentiation (Fig. 10C-G). In order to further clarify the role of CAA in inhibiting the adipocyte differentiation, the mRNA expression levels of genes encoding critical factors regulating adipose differentiation, including PPARγ, CCAAT enhancer binding protein α (C/EBP-α), adipocyte determination and differentiation factor 1/sterol regulatory element binding protein 1c (ADD1/SREBP1c), in addition to adipogenesis-related genes, including adipocyte fatty acid-binding protein 2 (AP2), lipoprotein lipase (LPL) and fatty acid synthase (FAS), were evaluated using RT-qPCR analysis following treatment with 50, 100, and 150 μM CAA for 8 days during differentiation. As shown in Fig. 11, compared with the cells without differentiation media, the expression levels of PPARγ, ADD1/SREBP1c, LPL (Fig. 11A), C/EBP-α, AP2 and FAS (Fig. 11B) were markedly increased in the cells in differentiation medium. However, treatment with CAA suppressed the mRNA levels of various adipogenic genes in a dose-dependent manner, which suggested that CAA treatment inhibited adipocyte differentiation by downregulating the adipogenic genes.

Discussion

Diabetes mellitus has become a prevalent metabolic disease worldwide (1). Insulin resistance and impaired insulin secretion are the principal causes of T2DM (18). Insulin resistance is a complex metabolic abnormality and is a common cause of concern in prediabetics and diabetics. It affects the ability of peripheral tissues to use insulin, thus impairs peripheral glucose utilization and results in the development of hyperglycemia and/or compensatory hyperinsulinemia (19).

Previous studies reported high expression levels of PTP1B in patients with T2DM and hyperlipidemia (10). PTP1B also regulates the activation of leptin and IR (5,7). Therefore, the present study investigated the ability of PTP1B to regulate insulin resistance. The results of the present study revealed that CAA functioned as an insulin sensitizer by inhibiting PTP1B. In addition, the results indicated that CAA treatment inhibited the activity of PTP1B and affected the expression of associated insulin signaling factors in the PTP1B overexpression-induced insulin resistance. Additionally, the CAA treatments used in the present study exhibited hypoglycemic and hypolipidemic effects *in vivo*. In the SD rats fed on a high-fat diet and with STZ-induced T2DM, treatment with CAA and
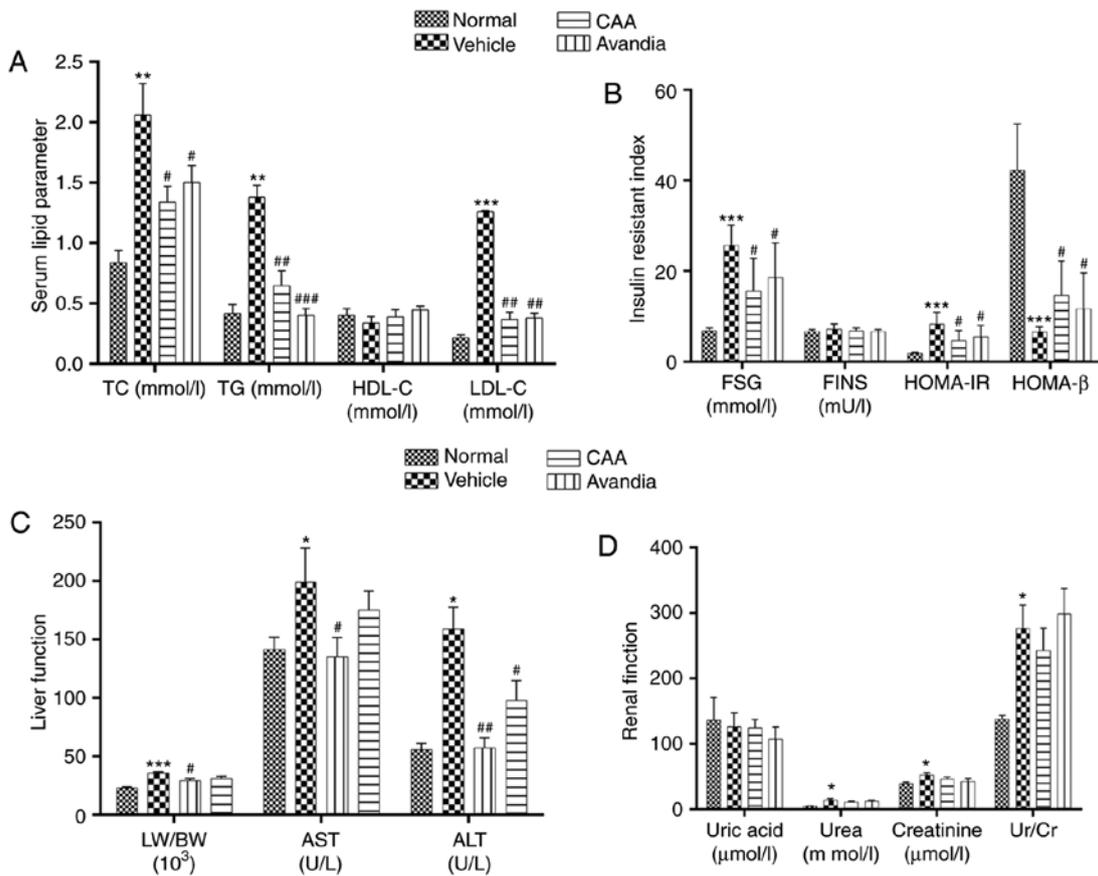
Figure 7. CAA lipid metabolism and organ function in type II diabetes mellitus rats. Blood samples were collected from the aorta abdominalis following 12 h of fasting at the end of the experiment. HOMA-IR and HOMA-β were calculated. The (A) serum lipid parameter, (B) insulin resistant index, (C) liver function and (D) renal function were analyzed using an automatic biochemical analyzer. Data are expressed as the mean ± standard error of the mean (n=8). *P<0.05, **P<0.01 and ***P<0.001, vs. normal rats; #P<0.05, ##P<0.01 and ###P<0.001, vs. vehicle-treated rats. CAA, cajanonic acid A; TC, total cholesterol; TG, triglycerides; HDL-C, high-density lipoprotein cholesterol; LDL-C, low-density lipoprotein cholesterol; FSG, fasting serum glucose; FINS, fasting insulin in serum; HOMA-IR, homeostatic model assessments for insulin resistance; HOMA-β, homeostatic model assessments for β-cell function; LW/BW, liver to body weight ratio; AST, aspartate transaminase; ALT, alanine transaminase; Ur/Cr, urea/creatinine ratio.
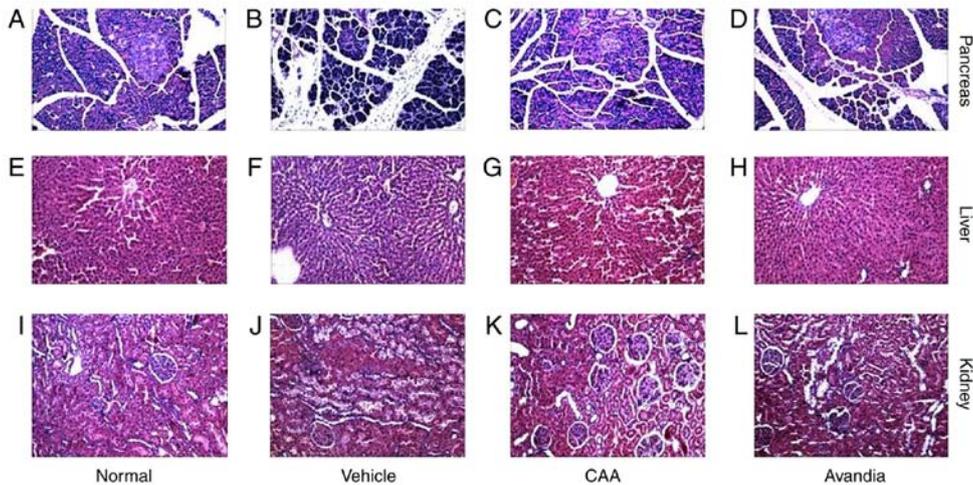
Figure 8. Histopathology of the pancreas, liver and kidneys by hematoxylin and eosin staining (magnification, x100). Pancreatic tissues from diabetic rats in the (A) normal, (B) vehicle, (C) CAA and (D) Avandia groups. Liver tissues of diabetic rats in the (E) normal, (F) vehicle, (G) CAA and (H) Avandia groups. Kidney tissues of diabetic rats in the (I) normal, (J) vehicle, (K) CAA and (L) Avandia groups. CAA, cajanonic acid A.

Avandia not only reduced blood glucose and lipid levels, but also protected the animals from organ damage. In the leptin-deficient *ob/ob* mice, which were congenitally obese and hyperglycemic, treatment with CAA reduced blood glucose and led to weight loss, showing the potential of CAA to treat obesity-associated diabetes.
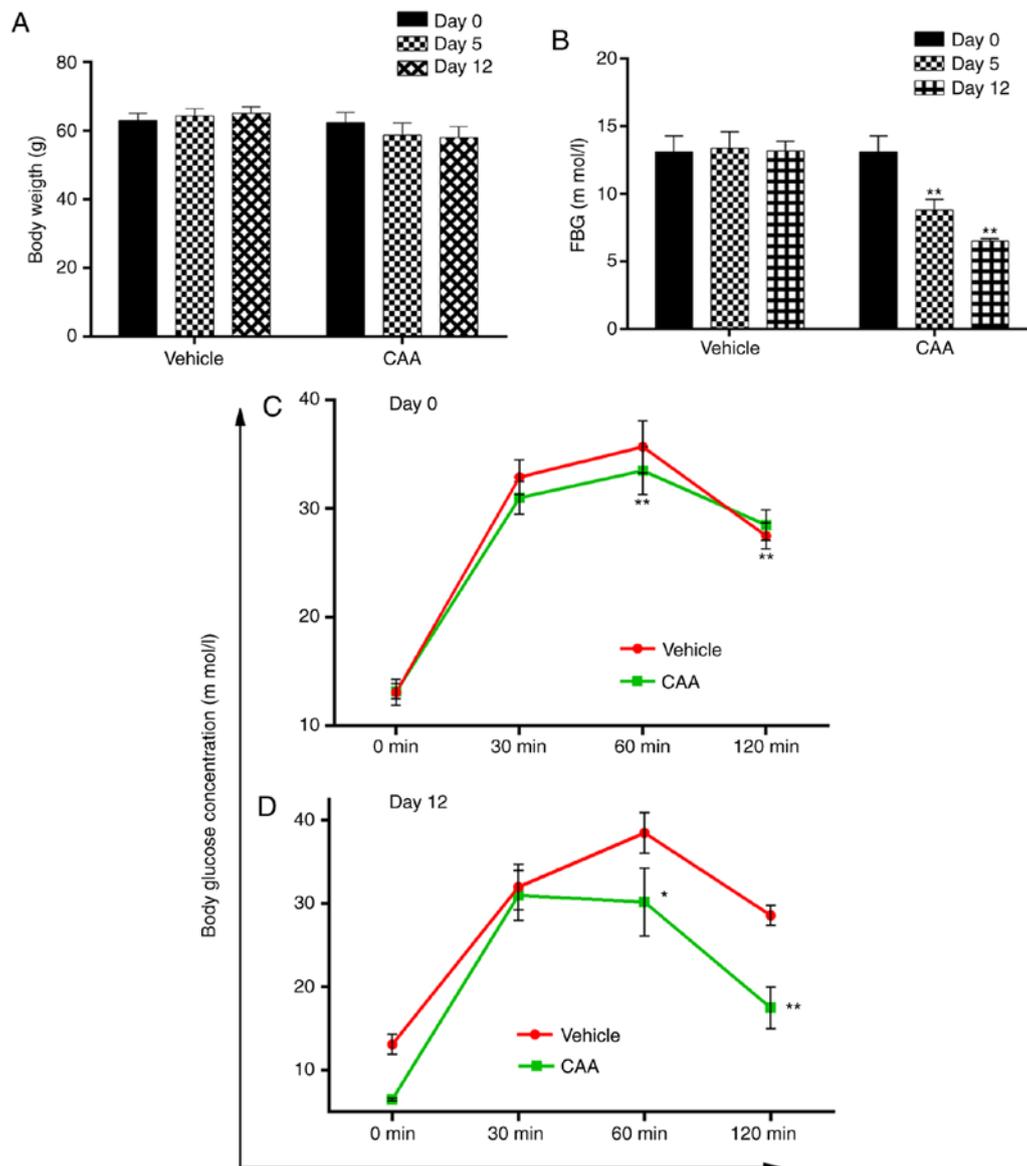
Figure 9. Anti-obesity and anti-hyperglycemic effects of CAA in *ob/ob* mice. Mice were administered with 8 mg/kg/day of CAA or vehicle for 12 days. (A) FBG and (B) BW were measured on days 0, 5 and 12. Oral glucose tolerance tests were performed in mice treated with CAA or vehicle on days 0 (C) and 12 (D). Data are expressed as the mean ± standard error of the mean (n=6). *P<0.05 and **P<0.01, vs. day 0. CAA, cajanonic acid A; FBG, fasting blood glucose.

The insulin signaling pathway is important in regulating glucose metabolism and maintaining glucose homeostasis. In target cells, the binding of extracellular insulin to the α-subunit of plasma membrane-located IR activates the β-subunit by autophosphorylation, which leads to the successive phosphorylation and activation of downstream signaling molecules, including IRS, PI3K and AKT (20). The activation of PI3K/AKT in adipose cells stimulates the translocation of intracellular GLUT4 vesicles to the membrane to transport glucose for storage. However, the activation of PI3K/AKT in liver cells promotes glycogen synthesis by inactivating GSK3β and increasing glucose transport by GLUT1 (21-23). The dephosphorylation of actively signaling molecules by the overexpression of PTP1B impairs insulin-stimulated signal transduction, which leads to a state of reduced glucose uptake, a condition known as insulin resistance (24). The findings of the present study were in accordance with this hypothesis, as the same results were observed in each of the PTP1B-transfected HepG2 cells, Dex-induced insulin-resistant HepG2 cells and 3T3-L1 adipocytes. In the present study, insulin alone was unable to promote the glucose consumption of cells overexpressing PTP1B; however, it was markedly increased in the presence of CAA, which indicated the ability of CAA to function as an insulin sensitizer. Mechanistic experiments revealed that CAA inhibited the activity and expression of PTP1B. CAA also increased the phosphorylation of IR, IRS1, PI3K and AKT, and the expression of GLUT1, in the insulin-resistant HepG2 cells. Additionally, CAA treatment increased the expression of GLUT4 in the insulin-resistant 3T3-L1 adipocytes, suggesting the potential of CAA to activate insulin signaling. In the present study, treatment with CAA reversed insulin sensitivity through the PI3K/AKT pathway by regulating the expression levels of IRS and GLUT *in vitro*. In addition, the mice lacking PTP1B
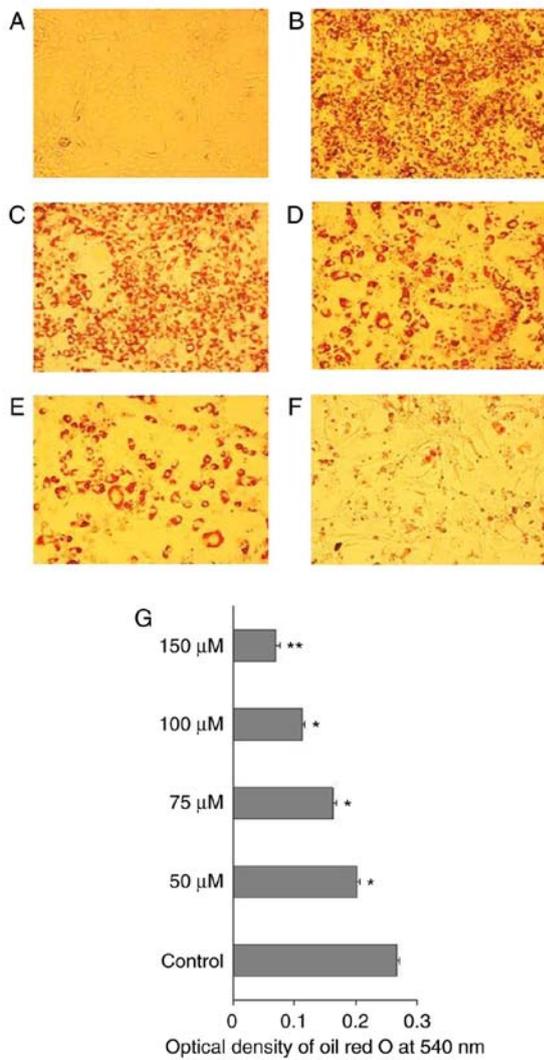
Figure 10. CAA inhibits hormone-induced 3T3-L1 preadipocyte differentiation. (A) 3T3-L1 preadipocytes were induced to differentiate in the (B) absence (control) or presence of (C) 50, (D) 75, (E) 100 or (F) 150 μM CAA. Mature adipocytes were stained using Oil Red O and analyzed under a microscope (magnification, x10). (G) Optical density of Oil Red O staining at 540 nm. The data from three independent experiments are expressed as the mean ± standard error of the mean (n=3). *P<0.05 and **P<0.01, vs. control. CAA, cajanonic acid A.

Figure 11. Effects of CAA on the expression of adipogenic genes in 3T3-L1 cells. Post-confluent 3T3-L1 preadipocytes were differentiated in the absence or presence of CAA for 8 days. mRNA expression levels of (A) PPARγ, ADD1, LPL and (B) C/EBPα, AP2 and FAS were measured using reverse transcription-quantitative polymerase chain reaction analysis. All the results are expressed as the mean ± standard error of the mean (n=6). *P<0.05 and **P<0.01. 1, 2 and 3 indicate CAA concentrations of 50, 100 and 150 μM, respectively. CAA, cajanonic acid A; PPAR, peroxisome proliferator-activated receptor γ; ADD1, adipocyte determination and differentiation factor 1; LPL, lipoprotein lipase; C/EBPα, CCAAT enhancer binding protein α; AP2, adipocyte fatty acid-binding protein 2; FAS, fatty acid synthase; DM, differentiation medium.

exhibited an advantage towards blood glucose homeostasis in specific tissues. The liver-specific downregulation of PTP1B in the mice resulted in enhanced glucose homeostasis and improved lipid profiles in liver, irrespective of the changes taking place in adiposity (25). In addition, treatment with CAA not only improved the functions of the liver, kidney and pancreas in the mice with T2DM, it also exerted a positive effect against T2DM. The HepG2 cell line was used in the present study, and this cell line has been demonstrated as a hepatoblastoma line (26). However, this misidentification is not likely to affect the outcomes or conclusions of the present study.

The expression of PTP1B has been reported to be key in regulating obesity (8,27,28). PTP1B$^{-/-}$ mice have been reported to produce reduced hepatic secretions of apolipoprotein B (apoB100) lipoproteins, one of the hallmarks of the lipid abnormalities of the metabolic syndrome (29). In the present study, the serum levels of TC (P<0.01), TG (P<0.01) and LDL-C (P<0.001) in the vehicle-treated T2DM rats were increased, and these factors were successfully reduced by CAA treatment. This indicated that CAA regulated the lipid metabolism via downregulating the expression of PTP1B. In addition, the efficacy of CAA in the congenitally obese and hyperglycemic *ob/ob* mice indicated the potential of CAA to treat obesity and obesity-induced metabolic disorder. PPARγ and C/EBPα are key transcription factors involved in adipocyte differentiation and adipogenesis. Their activity is essential for inducing adipogenesis. Furthermore, the transcription factor ADD1 can positively regulate the expression of PPARγ by binding to the *PPARγ* promoter (30), FAS, and LPL are typical factors in adipocyte differentiation and adipogenesis (31). Therefore, PPARγ, C/EBPα, ADD1/SREBP1c, AP2, Fas and LPL, were selected as indicators of lipid metabolism in the present study. CAA treatment in the present study inhibited adipocyte differentiation, accompanied by decreased mRNA levels of the adipogenic genes, including PPARγ, C/EBPα, ADD1/SREBP1c, AP2, FAS and LPL. These results indicated that the treatment with CAA decreased the expression of adipogenic genes, thus inhibited the adipocyte differentiation and adipogenesis in *ob/ob* mice by downregulating PPARγ (32). However, Avandia is a clinically used insulin sensitizer, which functions as a PPARγ

agonist. The results of the present study suggested that CAA also served as an insulin sensitizer, but that its mode of action was different from that of Avandia. Therefore, treatment of CAA may be used to restore insulin signaling transduction by inactivating PTP1B, and by downregulating PPARγ to avoid the side-effects of Avandia, including weight gain and fluid retention.

In conclusion, CAA treatment restored insulin signaling transduction by inhibiting the activity of PTP1B and activating insulin signaling transduction. Additionally, treatment with CAA was not only important in reducing blood glucose and preventing organ damage caused by hyperglycemia and hyperlipidemia, but also inhibited adipocyte differentiation and adipogenesis. The results of the present study indicated that CAA serves as a candidate for drug design and clinical applications and offers potential to restore insulin resistance and treat obesity-associated diabetes.

Acknowledgements

Availability of data and materials

The datasets used and/or analyzed during the current study are available from the corresponding author on reasonable request.

Authors' contributions

LW, JX, XL, SQ and SL performed the experiments and collected the data. XS, RY and YH conceived the study, performed the experiments, analyzed the data and wrote the paper with input from all authors.

Ethics approval and consent to participate

All experiments were approved by the Animal Ethics Committee of Guangzhou University of Chinese Medicine (no. SYXY2008-0001) and were performed following the Animal Care and Use guidelines set by the committee.

Patient consent for publication

Not applicable.

Competing interests

The authors declare that they have no competing interests.

References

1. Kahn BB: Type 2 diabetes: When insulin secretion fails to compensate for insulin resistance. Cell 92: 593-596, 1998.
2. Kahn SE, Hull RL and Utzschneider KM: Mechanisms linking obesity to insulin resistance and type 2 diabetes. Nature 444: 840-846, 2006.
3. Mayer-Davis EJ, D'Agostino R Jr, Karter AJ, Haffner SM, Rewers MJ, Saad M and Bergman RN: Intensity and amount of physical activity in relation to insulin sensitivity: The insulin resistance atherosclerosis study. JAMA 279: 669-674, 1998.
4. Kaur J: A comprehensive review on metabolic syndrome. Cardiol Res Pract 2014: 943162, 2014.
5. Ma YM, Tao RY, Liu Q, Li J, Tian JY, Zhang XL, Xiao ZY and Ye F: PTP1B inhibitor improves both insulin resistance and lipid abnormalities in vivo and in vitro. Mol Cell Biochem 357: 65-72, 2011.
6. Seely BL, Staubs PA, Reichart DR, Berhanu P, Milarski KL, Saltiel AR, Kusari J and Olefsky JM: Protein tyrosine phosphatase 1B interacts with the activated insulin receptor. Diabetes 45: 1379-1385, 1996.
7. Knobler H and Elson A: Metabolic regulation by protein tyrosine phosphatases. J Biomed Res 28: 157-168, 2014.
8. Elchebly M, Payette P, Michaliszyn E, Cromlish W, Collins S, Loy AL, Normandin D, Cheng A, Himms-Hagen J, Chan CC, et al: Increased insulin sensitivity and obesity resistance in mice lacking the protein tyrosine phosphatase-1B gene. Science 283: 1544-1548, 1999.
9. Klaman LD, Boss O, Peroni OD, Kim JK, Martino JL, Zabolotny JM, Moghal N, Lubkin M, Kim YB, Sharpe A, et al: Increased energy expenditure, decreased adiposity, and tissue-specific insulin sensitivity in protein-tyrosine phosphatase 1B-deficient mice. Mol Cell Biol 20: 5479-5489, 2000.
10. Koren S and Fantus IG: Inhibition of the protein tyrosine phosphatase PTP1B: Potential therapy for obesity, insulin resistance and type-2 diabetes mellitus. Best Pract Res Clin Endocrinol Metab 21: 621-640, 2007.
11. Sun C, Zhang F, Ge X, Yan T, Chen X, Shi X and Zhai Q: SIRT1 improves insulin sensitivity under insulin-resistant conditions by repressing PTP1B. Cell Metab 6: 307-319, 2007.
12. Obanda DN and Cefalu WT: Modulation of cellular insulin signaling and PTP1B effects by lipid metabolites in skeletal muscle cells. J Nutr Biochem 24: 1529-1537, 2013.
13. Qiu SX and Shen XL: A hypoglycemic and slimming stilbenoidal natureal medicine. CN Patent 101422450. Filed October 9, 2008; issued May 6, 2009.
14. Cai JZ, Tang R, Ye GF, Qiu SX, Zhang NL, Hu YJ and Shen XL: A Halogen-containing stilbene derivative from the leaves of Cajanus cajan that induces osteogenic differentiation of human mesenchymal stem cells. Molecules 20: 10839-10847, 2015.
15. Yuan J, Lin J, Xu C, Ye Q, Xiong Y, Huang L and Yuan H: Experimental research on prevention of glucocorticoid-induced avascular necrosis of the femoral head with tongluo shenggu capsule. Tradit Chin Drug Res Clin Pharmacol 16: 185-188, 2005 (In Chinese).
16. Livak KJ and Schmittgen TD: Analysis of relative gene expression data using real-time quantitative PCR and the 2(-delta delta C(T)) method. Methods 25: 402-408, 2001.
17. Samuel VT, Petersen KF and Shulman GI: Lipid-induced insulin resistance: Unravelling the mechanism. Lancet 375: 2267-2277, 2010.
18. Nandi A, Kitamura Y, Kahn CR and Accili D: Mouse models of insulin resistance. Physiol Rev 84: 623-647, 2004.
19. Duque-Guimaraes DE and Ozanne SE: Nutritional programming of insulin resistance: Causes and consequences. Trends Endocrinol Metab 24: 525-535, 2013.
20. Krook A, Wallberg-Henriksson H and Zierath JR: Sending the signal: molecular mechanisms regulating glucose uptake. Med Sci Sports Exerc 36: 1212-1217, 2004.
21. Huang S and Czech MP: The GLUT4 glucose transporter. Cell Metab 5: 237-252, 2007.
22. Lochhead P, Coghlan M, Rice S and Sutherland C: Inhibition of GSK-3 selectively reduces glucose-6-phosphatase and phosphatase and phosphoenolypyruvate carboxykinase gene expression. Diabetes 50: 937-946, 2001.
23. Chi YJ, Li J, Guan YF and Yang JC: PI3K/Akt signaling axis in regulation of glucose homeostasis. Chin J Biochem Mol Biol 26: 879-885, 2010 (In Chinese).
24. Bhattacharya S, Dey D and Roy SS: Molecular mechanism of insulin resistance. J Biosci 32: 405-413, 2002.

25. Delibegovic M, Zimmer D, Kauffman C, Rak K, Hong EG, Cho YR, Kim JK, Kahn BB, Neel BG and Bence KK: Liver-specific deletion of protein-tyrosine phosphatase 1B (PTP1B) improves metabolic syndrome and attenuates diet-induced endoplasmic reticulum stress. Diabetes 58: 590-599, 2009.
26. López-Terrada D, Cheung SW, Finegold MJ and Knowles BB: Hep G2 is a hepatoblastoma-derived cell line. Hum Pathol 40: 1512-1515, 2009.
27. Cheng A, Uetani N, Simoncic PD, Chaubey VP, Lee-Loy A, McGlade CJ, Kennedy BP and Tremblay ML: Attenuation of leptin action and regulation of obesity by protein tyrosine phosphatase 1B. Dev Cell 2: 497-503, 2002.
28. Bence KK, Delibegovic M, Xue B, Gorgun CZ, Hotamisligil GS, Neel BG and Kahn BB: Neuronal PTP1B regulates body weight, adiposity and leptin action. Nat Med 12: 917-924, 2006.
29. Goldstein BJ: Regulation of insulin receptor signaling by protein-tyrosine dephosphorylation. Receptor 3: 1-15, 1993.
30. Lee JE and Ge K: Transcriptional and epigenetic regulation of PPARγ expression during adipogenesis. Cell Biosci 4: 1-11, 2014.
31. Song DD, Chen Y, Li ZY, Guan YF, Zou DJ and Miao CY: Protein tyrosine phosphatase 1B inhibits adipocyte differentiation and mediates TNFα action in obesity. Biochim Biophys Acta 1831: 1368-1376, 2013.
32. Gregoire FM, Smas CM and Sul HS: Understanding adipocyte differentiation. Physiol Rev 78: 783-809, 1998.